Journal of Cellular Biochemistry 18:363-375 (1982)

Structural Characteristics of the Short-Tail Fibers of T4 Bacteriophage

Jorge Zorzopulos, Sara DeLong, Virginia Chapman, and Lloyd M. Kozloff

University of Colorado Health Sciences Center, Denver, Colorado 80262

The characteristics of pure preparations of short-tail fibers of bacteriophage T4 have been studied in the optical and electron microscope. Three main structures were observed: 1) spheres of 8.1 nm diameter; 2) fibers 43 nm long and 3.8 nm thick; and 3) fibers 54 nm long and 3.2 nm thick. Both types of fibers exhibited a regular beaded appearance. The 43-nm fibers were the most abundant structure. During the process of purification of the short-tail fibers, the formation of aggregates was observed each time the material containing the short-tail fibers was dialyzed against saline solutions. These aggregates became increasingly fibrous (as observed in the optical microscope) as the material used was increasingly enriched in short-tail fibers. Finally, most of the aggregates were of the fibrous type when they were formed from a purified preparation of short-tail fibers. In the electron microscope, it was found that the filamentous aggregates were organized in well-defined bundles. The amino acid composition of the highly purified short-tail fibers was also determined. Among the known fibrous proteins, the ones that most resemble the amino acid composition of the short-tail fibers are actin and fibrinogen. These observations are discussed in relation to the T4 short-tail fiber structure and their localization on the hexagonal baseplate of the T4 tail structure.

Key words: T4 bacteriophage, short-tail fibers, fiber formation

The baseplate substructure of the tail of Escherichia coli bacteriophage T4 particle is composed of at least 14 proteins in a flat hexagonal arrangement [1]. Two different attachment appendixes protrude from these hexagons, which have been called the long-tail fibers and the short-tail fibers [2,3]. The short-tail fibers have been shown to be trimeric proteins whose monomer is the product of gene 12 (gP12) of the phage genome [4]. The molecular weight of gP12 monomer is about 55,000 daltons [4], and when it is in the trimer form as the short-tail fiber, it has three tightly bound Zn^{2+} ions [5]. Many of the properties of the short-tail fibers have been investigated by Haselkorn and his colleagues [4,6,7]. They have reported that the short-tail fibers are about 35 nm long and 3–4 nm thick and that they display a characteristic beaded appearance when observed in the electron microscope. This report describes: 1) modifications of the purification procedure for the short-tail fibers originally described by Mason and Haselkorn [4], which increase the final

Jorge Zorzopulos and Lloyd M. Kozloff are now at the Department of Microbiology and Immunology, University of California, San Francisco, CA 94143.

Received February 5, 1981; accepted October 10, 1981.

0730-2312/82/1803-0363$04.00

yield; 2) the different structures observed in a purified preparation of short-tail fibers in the electron microscope as well as their relative distribution; 3) the formation of characteristic filaments upon polymerization of the short-tail fibers; and 4) the amino acid composition of the short-tail fibers. A preliminary report of some of these results has been presented [8].

MATERIALS AND METHODS

Bacterial and Phage Strains and Growth Conditions

E coli strains B and CR63 served as the nonpermissive and permissive host, respectively, for bacteriophage T4 and various T4 amber mutants. The growth and assay of these virus stocks were performed by standard procedures [9]. The T4D amber mutants used were a baseplate minus mutant, 54^- (H21), a head minus mutant, 23^- (B17), and a short-tail fiber minus mutant, 12^- (N69) all obtained from the original stocks of Edgar and Wood [10]. The bacteria were grown in tryptone broth media containing 8 gm of tryptone (Difco) and 5 gm of NaCl per liter.

Purification of the Short-Tail Fibers

A modification of the method described by Mason and Haselkorn [4] was used. T4D 54am infected E Coli B or T4D 23am infected E coli B was the source of the short-tail fibers. The cells were grown at 37°C with vigorous aeration until the cell concentration was 4×10^8 cells/ml. At this time, the cells were infected at a multiplicity of four phage/bacterium and reinfected 10 min later with the same multiplicity. The cells were incubated at 37°C for 100 min and then centrifuged at 1000g for 15 min in the cold. The pellet, usually from 2 liters, was resuspended in 10 ml of a buffer containing 0.06 M sodium phosphate, pH 7.0, and sonicated (nine pulses of 30 sec each with cooling between each pulse using a Branson S125 sonifier). Subsequently, 0.5 mg of DNase was added, and the suspension was incubated for 15 min at 30°C and was then centrifuged at 27,000g for 60 min in the cold. The pellet was resuspended in 10 ml of 0.06 M phosphate buffer, pH 7.0, containing 10 mM EDTA and incubated 30 to 60 min at room temperature. Then the suspension was centrifuged, first for 15 min at 3,000g to remove debris, and then the supernatant solution was centrifuged again for 90 min at 27,000g in the cold. The resulting supernatant solution contained a number of proteins but was rich in short-tail fibers. Twenty-four milliliters of this supernatant solution was loaded on top of 10 ml of 20% sucrose in 0.06 M phosphate buffer containing 0.01 M EDTA. The tubes were centrifuged for 41 h at 27,000 rpm in a Beckman model L-2 ultracentrifuge using a S.W. 25.1 rotor. After the centrifugation, ten equal fractions were collected and the pellet resuspended in a volume of buffer equal to the volume of the individual fractions. The fractions were analyzed for their content of short-tail fibers by SDS-PAGE as described below. The fractions enriched in short-tail fibers were pooled and dialyzed against phosphate buffer 0.06 M, pH 7.0, containing 0.01 M EDTA. The dialysis bag was then exposed to a gentle air current in the cold. When the volume was reduced to 10% of the original volume, the solution was chromatographed upwards using a peristaltic pump through a Sephadex G200 column that was 3.2 cm × 96 cm. The elution buffer was 0.06 M phosphate, pH 7.0, containing 0.01 M EDTA. The total elution volume was 500 ml, and the fractions were each of 13 ml. Each fraction was analyzed for its short-tail fiber content by a biological complementation reaction, for protein content by tryptophan fluorescence, and for

purity by SDS-PAGE analysis (see below). The fractions containing the largest biological complementation activity and giving only one protein band in the SDS-PAGE analysis were used as the purified short-tail fibers preparation.

Filament Formation

Preparations from different steps of the purification process of the short-tail fibers were dialyzed against a solution containing 0.06 M KCl and 0.02 $MgSO_4$ (unless otherwise stated). Then the dialysis bag was exposed to a gentle air current in the cold, and the concentration was allowed to procede until many large aggregates were observed. These aggregates were separated by centrifugation at 9,000g for 4 min in a Beckman microfuge B. The supernatant solution was usually concentrated again to obtain more aggregates. The aggregates were resuspended in sodium acetate buffer 0.1 M, pH 6.8. This preparation was used for electron microscope observation and SDS-PAGE analysis.

Gel Electrophoresis

Denaturing gel electrophoresis was carried out on slab gels containing 10% acrylamide, 0.27% bis-acrylamide, 0.1% SDS. The running buffer was 0.012 M Trizma Base, 0.1 M glycine, pH 8.8, with 0.1% SDS. Protein bands were stained with Coomassie blue. Phosphorylase b (94 K), bovine serum albumin (67 K), ovalbumin (43 K), and carbonic anhydrase (30 K) were used as molecular weight standards.

Electron Microscopy

Samples were prepared for electron microscopy by negative staining with a saturated solution of uranyl acetate in water on carbon-coated copper collodion grids. They were examined and photographed with an R.C.A. E.M.U. 4 electron microscope.

Complementation Reaction

Two hundred microliters of the Sephadex G200 column fractions were incubated with 20 μl of an extract of E coli B infected with a T4D 12^- amber mutant and with 50 μl of a buffer containing 0.004 M K_2HPO_4, 0.002 M KH_2PO_4, 0.007 M NaCl, and 0.02 M $MgSO_4$, pH 7.4. The mixture was incubated overnight at 30°C. After that, different dilutions of the mixture were assayed for plaque formation using E coli CR63 as the indicator bacteria.

Protein Determination and Amino Acid Analysis

Protein was measured against a crystalline bovine serum albumin standard solution in an Aminco-Bowman spectrophotofluorometer at an excitation wavelength of 280 nm and emission at 340 nm. Amino acid analysis was carried out by standard procedures using a DURUM type amino acid analyzer.

RESULTS

Purification of the T4 Short-Tail Fibers

The purification of the T4 short-tail fibers (called STF) followed the general lines of the procedure described by Mason and Haselkorn [4], but modifications were introduced to increase the final yield. The most important modification was to

avoid the use of ammonium sulfate precipitation since it caused the formation of aggregates. Many of these aggregates were not dissolved upon removal of the ammonium sulfate by dialysis. The SDS-PAGE analysis of these aggregates boiled in a buffer containing 2% SDS as indicated in Materials and Methods showed that they contain large amounts of STF. This was the first indication that STF tended to form polymeric structures.

Figures 1, 2, and 3 show SDS-PAGE analysis of some of the last steps in the purification of the T4 STF. Figure 1A shows the pattern of proteins extracted with EDTA from the debris of E coli B cells infected with a 12^- mutant (gel A) and a 12^+ mutant (gel B). As can be seen, a well-defined band of about 55,000 daltons is present in these preparations when the bacteria was infected with a 12^+ mutant. This protein was absent from the preparation if the bacteria were infected with a 12^- mutant. This protein is known to be the subunit of the T4 short-tail fibers and to be the product of the T4 gene 12 (gP12) [4]. Figure 2 shows gels of the fractions re-

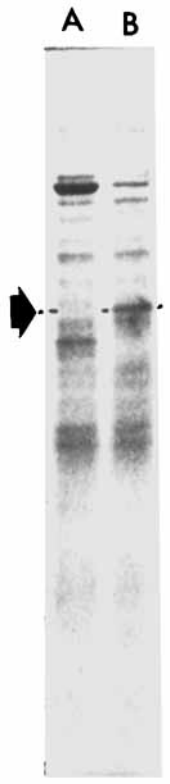

Fig. 1. Coomassie blue-stained SDS-PAGE analysis (10% acrylamide) of a crude STF preparation. The samples are: A, proteins extracted with 0.01 M EDTA from debris of E coli B cells infected with 12^- T4 amber mutant. B, same as in A but the E coli B cells were infected with 54^- amber mutant. The arrow indicates the position of gP12, the protein subunit of the STF.

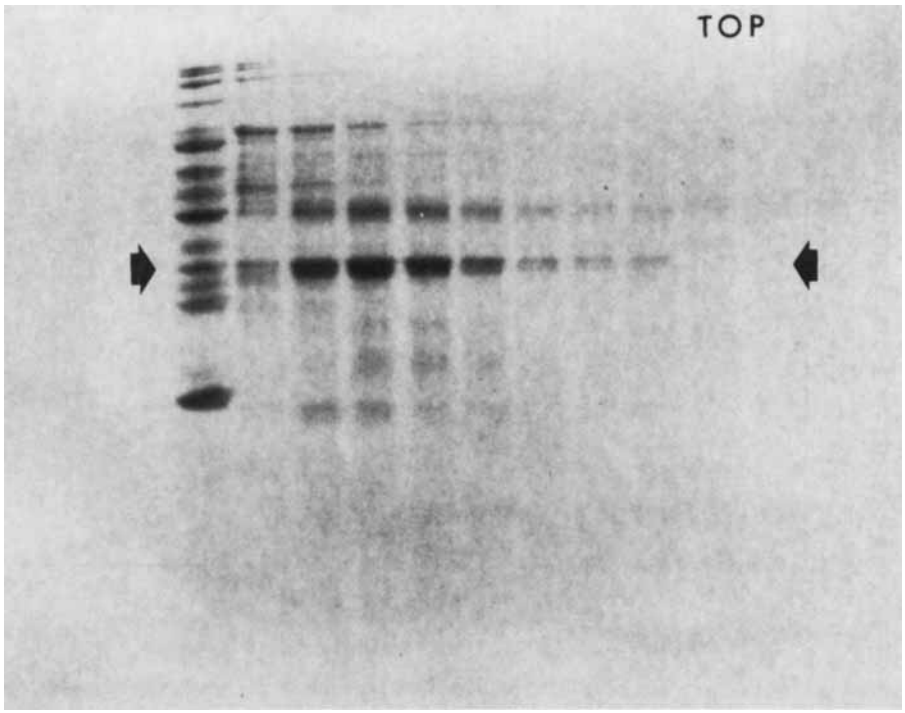

Fig. 2. SDS-PAGE analysis of the fractions obtained after centrifugation in a sucrose gradient of the proteins extracted with EDTA from debris of E coli B cells infected with a 54⁻ amber mutant. The conditions of the centrifugation has been described in Materials and Methods. The arrow indicates the position of gP12.

sulting from a sucrose gradient fractionation of the proteins extracted by EDTA as described in Materials and Methods; the presence of the STF was determined by the presence of gP12 in these gels. Figure 3 shows the elution position of the STF when the fractions of the sucrose gradient rich in STF were pooled, concentrated, and passed through a G200 Sephadex column as indicated in Materials and Methods. The position of the STF was determined by the complementation activity found for each Sephadex column fraction upon incubation with a crude extract of E coli B infected with a T4 12⁻ amber mutant. The SDS-PAGE analysis of the fractions with largest complementation activity shows that the STF was the only protein present in these fractions in significant amounts (see insert on Figure 3), and this preparation was used for the following experiments.

Electron Microscopy of the STF

In agreement with the findings reported by Kells et al [7], most of the STF show a characteristic beaded appearance when observed in the electron microscope (Fig. 4). Most of the fibers have a length close to 43 nm (Fig. 5B) and a diameter of about 3.8 nm. This length is longer than the mean length of 36 nm reported by Kells

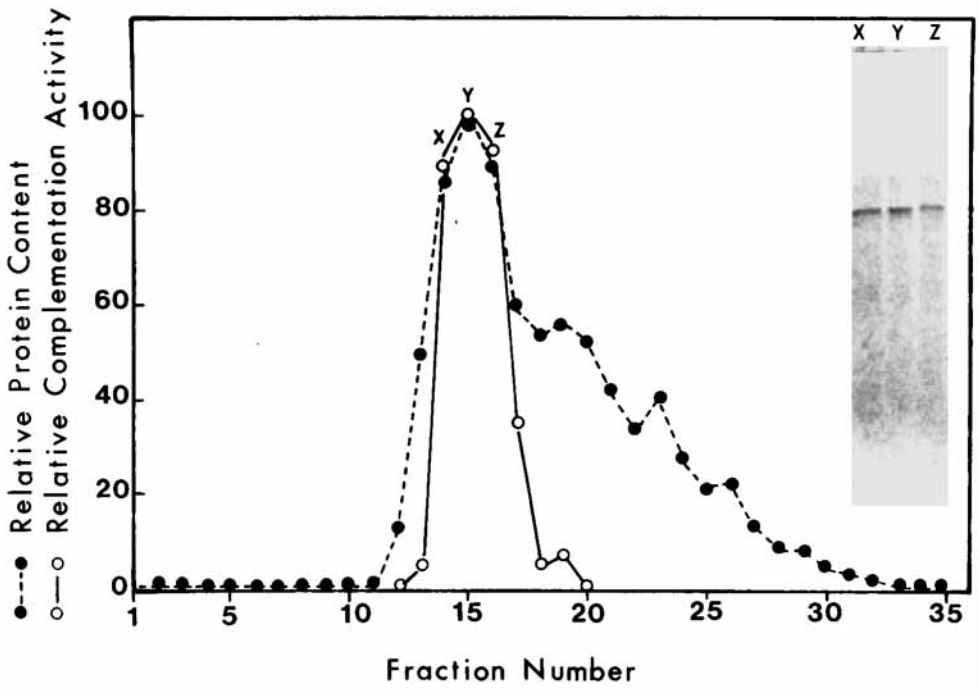

Fig. 3. Fractionation on a Sephadex G200 column of the pooled STF-rich fractions obtained by centrifugation in a sucrose gradient fraction. Conditions for the chromotographic procedure and complementation assay have been described in Materials and Methods. Insertions: SDS-PAGE protein patterns of the fractions No. 14, 15, and 16 of the Sephadex G200 column.

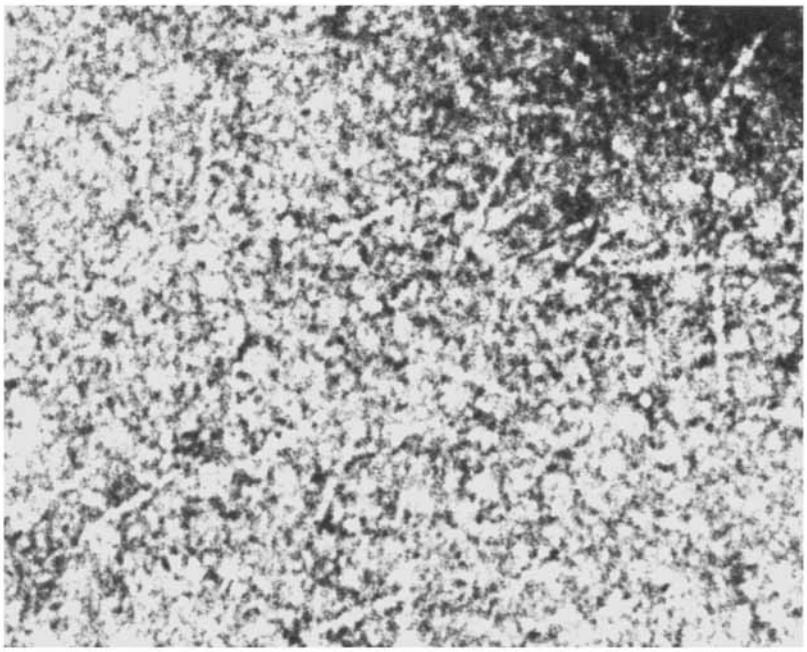

Fig. 4. Electron micrograph of the purified short-tail fiber preparation. Magnification × 370,000.

et al [7]. Our measurements were done using T4 particles as internal standards and taking the length of the main phage tail as 95 nm. In our preparations, we also observed longer fibers. Their lengths were about 54 nm (Fig. 5C); they also had regular beads, but the diameter of the beads was smaller than the beads of the 43 nm fibers (about 3.2 nm). Therefore, it appears that these fibers are more stretched. Finally, other structures observed were spheres of about 8.1 nm in diameter (Fig. 5A). They had a small indentation in the middle area. Figure 6 shows a distribution of the fibers according to their length and their relative abundance in our preparations. It can be seen that although the 43 nm fibers are by far the most abundant structure, there is a significant amount of both spheres, 8.1 in diameter, and stretched fibers of 54 nm.

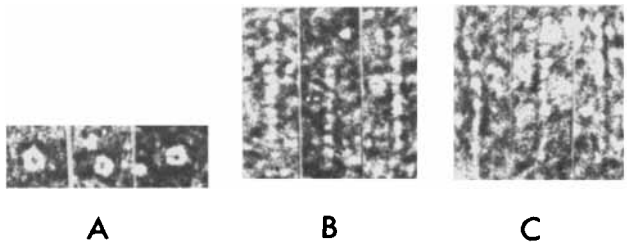

Fig. 5. Electron micrographs of the different structures founded in the purified STF preparation. Magnification × 370,000. A is the spheres, and B and C are the two fibers of different lengths.

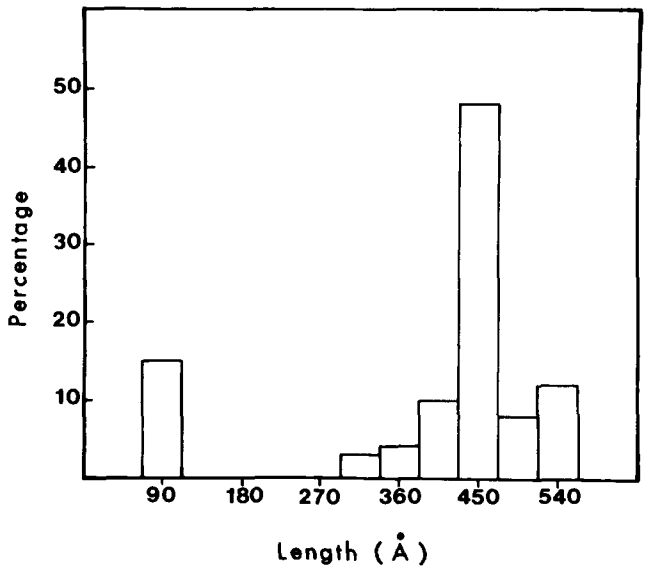

Fig. 6. Length distribution of the different structures observed in electron micrographs of the purified STF preparation. These percentages were obtained by measurement of a total of 600 fibers.

Filament Formation

It has been pointed out above that during the purification of the STF, it was observed that precipitation with $(NH_4)_2SO_4$ produced the formation of aggregates. Other conditions where the formation of aggregates were observed were 1) dialysis against water of the proteins extracted with EDTA from debris of E coli B infected with T4 amber mutants, 2) dialysis of the same EDTA-extracted proteins against 0.06 M KCl, 3) dialysis of the same preparation against 0.02 M $MgSO_4$; and 4) dialysis of the same preparation against KCl 0.06 M and 0.02 M $MgSO_4$. In all these conditions, aggregate formation was increased by concentrating the dialyzed protein. The poorest aggregate formation was obtained by dialysis of the STF preparations against water, and the best results were obtained by dialysis against KCl and $MgSO_4$ simultaneously. In all these cases, the analysis of aggregates by SDS-PAGE demonstrated large amounts of STF as components of these aggregates. Similar results were obtained using a pool of the STF-enriched fractions obtained from the

Fig. 7. SDS-PAGE analysis of purified STF. The samples are: A, proteins present in the aggregates obtained as a result of the dialysis against 0.02 M $MgSO_4$ and 0.06 M KCl of the pooled sucrose gradient fractions rich in STF (see Fig. 2) and B, proteins present in the aggregates obtained as a result of the dialysis of the purified STF preparation against 0.02 M $MgSO_4$ and 0.06 M KCl.

sucrose gradient used during the STF purification. Figure 7A shows the SDS-PAGE analysis of aggregates formed during the dialysis of the pooled sucrose-gradient fractions against 0.02 M $MgSO_4$ and 0.06 M KCl. It was found that the main component of these aggregates was the protein subunit of the STF (gP12). Furthermore, if the purified STF preparation obtained after the final step of purification through the Sephadex G200 column was dialyzed against 0.02 M $MgSO_4$ and 0.06 M KCl, the formation of aggregates was again observed (Fig. 7B). The optical microscope observations showed that the percentage of the aggregates displaying fibrous characteristics increased as the preparation used was increased in its relative STF content, and, finally, when the pure STF preparation was used, most of the aggregates formed were of fibrous type (Fig. 8). A similar correlation of aggregate formation was also observed in the electron microscope. Amorphous aggregates were frequently seen when the preparation used was rich in other proteins besides STF (Fig. 9A), but very well-defined filament bundles were only observed when the aggregates were obtained from the dialysis against $MgSO_4$ and KCl of the purified preparation of STF (Fig. 9B,C,D).

Amino Acid Composition of STF

Table I shows the amino acid composition of the STF. There is a clear difference in the relative amino acid composition of the T4 STF as compared with other groups of fibrous proteins like silk, flagellin, elastin, resilin, collagen, high sulfur keratins, myosin, tropomyosin, and paramyosin [11]. There is a small similarity between the amino acid composition of the short-tail fibers [12] as well as with intermediate filaments isolated from different sources [13]. The resemblance in amino

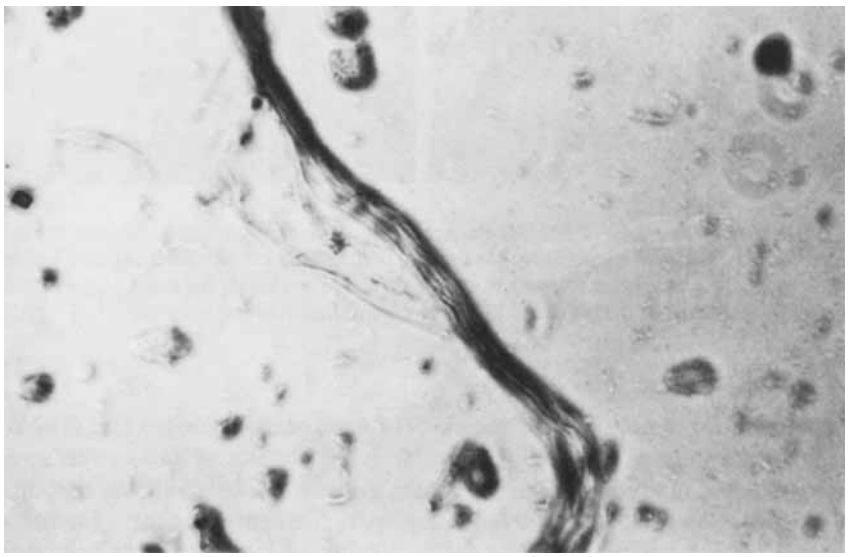

Fig. 8. Optical microscope photograph of the fibrous structures formed as a result of the dialysis against 0.02 M $MgSO_4$ and 0.06 M KCl of the purified STF preparation. Magnification × 1300.

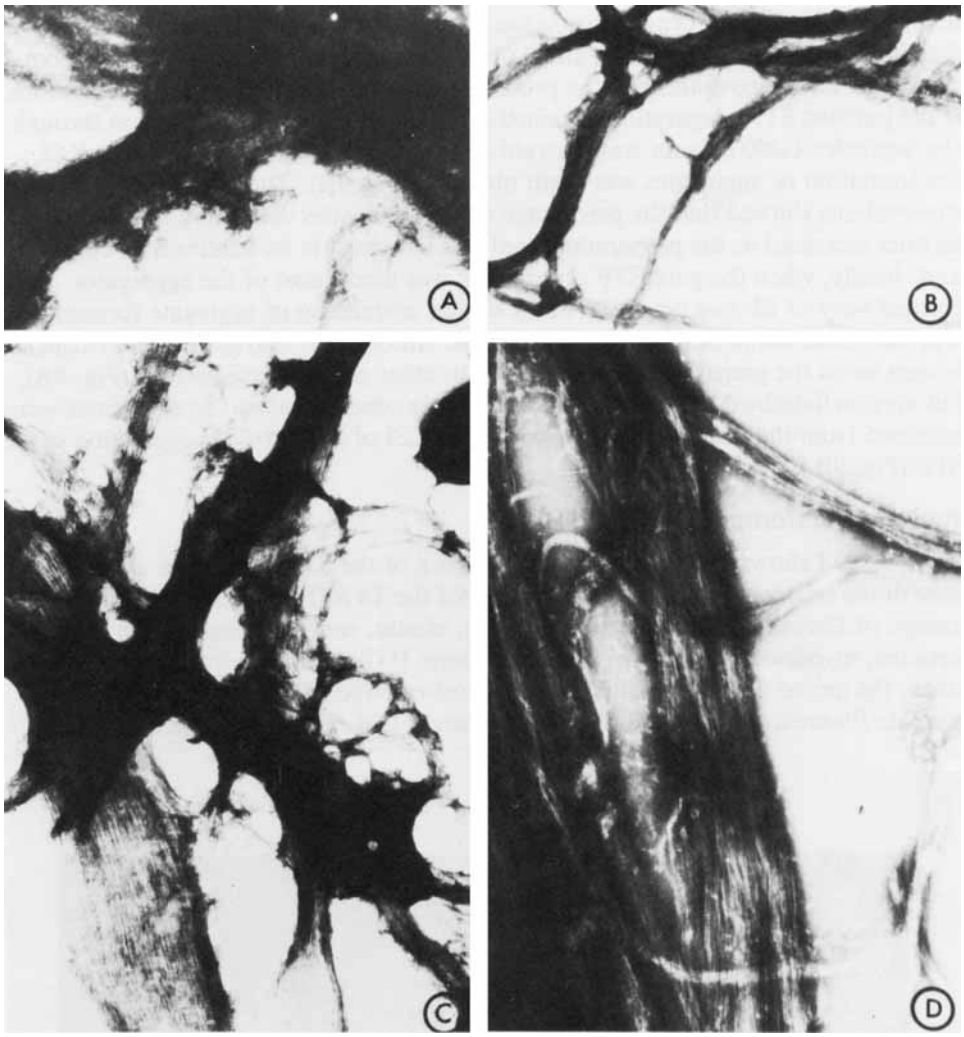

Fig. 9. Electron micrographs of STF. The samples are: A, amorphous aggregates observed as contaminants of the fibrous structures when the original preparations contain other proteins besides STF, and B, C and D, well-organized filament bundles obtained as a result of the dialysis against 0.02 M $MgSO_4$ and 0.06 M KCl of the purified STF preparation. Magnification × 39,000.

acid composition is strongest for the cases of actin and fibrinogen [11] (Table I). The main difference as compared with actin is the content of half-cystine and methionine, while the main differences as compared with fibrinogen is the content of alanine, lysine, and half-cystine. Actin can form filaments, but these filaments have a distinctive characteristic as compared with other animal cell filaments in that they possess a low content of both α-helix and β-sheet configurations and appear to be more like a random coil [11]. The content of proline and glycine in actin is greater than the usual content of these amino acids in highly helical proteins like tro-

TABLE I. Amino Acid Composition of T4 Short-Tail Fibers as Compared With Actin and Fibrinogen (% Composition)*

Amino acid	Short-tail fibers	Actin	Fibrinogen
Alanine	9.2	8.0	4.9
Arginine	5.2	4.8	5.4
Aspartic acid	10.5	9.0	12.4
Glutamic acid	10.5	11.3	11.4
Glycine	9.8	7.5	10.0
Half-cystine	0.15	1.4	2.5
Histidine	2.9	2.0	2.0
Isoleucine	5.7	7.6	4.0
Leucine	7.4	7.0	6.1
Lysine	4.6	5.4	7.4
Methionine	2.1	4.1	2.2
Phenylalanine	3.2	3.1	3.4
Proline	4.5	4.9	4.8
Serine	6.6	5.9	7.0
Threonine	7.6	6.9	6.1
Tyrosine	3.1	4.0	3.5
Valine	7.1	5.4	5.0

*The amino acid analysis of the STF was kindly performed by Dr. W. Hirs. The values for actin and fibrinogen were taken from Johnson and Perry [25] and from McKee et al [26], respectively.

pomyosin and paramyosin [11]. It has been postulated that this difference in the content of proline and glycine may account for its low content of α-helix [11]. It should be noted that the combined proline and glycine content of actin is 12.4%, while the short tail fibers possess an even higher combined content of these two amino acids of 14.3%.

DISCUSSION

A number of steps precedes the phage DNA injection into the host cytoplasm during the infection with T4 phage. The first step is the attachment of the phage long-tail fibers to the host cell receptors. After that, the phage baseplate approaches the host cell wall and the short-tail fibers are then able to find their own receptor sites. It is at this moment that a number of important modifications of the tail of the phage particle takes place. The baseplate, a hexagonal substructure of the phage infectious particle undergoes a transition to a star-like configuration [1]. A central hole appears in the baseplate and through which the tail tube of T4, a conduit for the DNA, passes on its way through the host cell wall [2]. Simultaneously, the T4 tail sheath contracts. At this time, the short-tail fibers appear as fibers about 40 nm long connecting the six vertices of the baseplate with the host cell wall [2]. However, the molecular configuration of the short-tail fibers on the infective particle where the baseplate still has a hexagonal arrangement is still unknown. Based on the different configurations observed in the STF purified preparations (Fig. 5), a proposal can be made about the organization of the short-tail fibers. The highly condensed spherical structure is a good candidate for the original configuration of the STF on the hexagonal baseplate. Figure 10 shows a superposition of one of these spherical structures on a T4 hexagonal baseplate. Both structures were taken from electron micrographs at the same magnification. It is evident that six of these spheres could

be arranged in a radial fashion on the baseplate. Further, each STF would be in close contact with gP11, the protein that makes up the distal portion of the baseplate tail pins [1]. This arrangement is in agreement with the fact that the STF can be added to the baseplate only after gP11 has been incorporated [14,15]. On the other hand, Crowther et al [1] has observed in lateral views of the T4 tails that gP12 formed a bridge between the pins. It is easy to see that this image would be the one projected by the junction of two spheres as proposed in Figure 10. Finally, there is indirect evidence indicating that the STF may be one element that is able to interconnect the tail pins to the central plug of the baseplate because, in addition to the fact that they are in contact with gP11, they seem to be also in contact with gP5 [16], a component of the central tail plug. This interconnection as well as other forces [17] may be of importance in the stabilization of the baseplate in the hexagonal configuration. Upon binding of the short-tail fibers to its receptor on the host cells, these connections could be broken allowing the transition to the star configuration. This proposal is in agreement with the fact that the star configuration is the one favored in baseplates that lack gP12 [1].

Filament formation by purified T4 short-tail fibers deserves comment. Recently, there have been several papers describing the presence of filaments or the formation of filament by proteins coded for by the genomes of lower organisms [18–22]. It also has been put forward that "actin" is a component of the envelope of some animal viruses [23], but in this case, the protein is coded for by the cell host and is incorporated into the virus during the wrapping of the nucleus capsid. To our knowledge, this work on gP12 is the first report of a true viral protein that is able to form filaments similar to some animal cell filaments. Filaments as well as the filament bundles have been successfully used in the past for the investigation of the structure of the protein structure by X-rays as well as by optical diffraction [11]. We hope in the future to learn more about the T4 short-tail fiber structure through the analysis of such filaments. Currently, the fact that the STF are able to form actin-like filaments, as well as the results from the amino acid composition and early studies on its trimeric nature [4], favors a model where the STF are formed by three polypeptides that intertwine forming a regular succession of globular structures

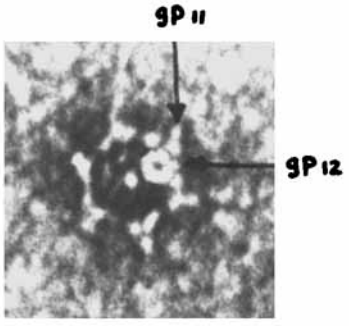

Fig. 10. Superposition of one of the spherical structures observed in purified STF preparations under the electron microscope to an electron micrograph of a T4 baseplate. Magnification × 500,000.

(beading) in a disposition similar to the one found for the globular subunit of F-actin [24]. However, each globular subunit in the case of the short-tail fibers will be smaller than the globular subunit of F-actin, since the total molecular weight of the short-tail fiber is about 165,000 daltons, and each short-tail fiber exhibits about eight globular bead-like structures that gives a molecular weight of about 21,000 for the globular elements as compared with about 42,000 daltons for the F-actin globular elements. If the molecular density is considered to be the same for both proteins and the diameter of the bead-like element of actin is taken as 5.5 nm [11], it can be calculated that the diameter of the globular element of the STF would be 3.9 nm in good agreement with diameter reported by Kells et al [17] and found in this work. The STF stretched structure with a length of 54 nm observed in the electron microscope may approach a configuration resembling a three-strand coiled-coil rope. However, from the molecular weight of the subunit of the STF (55,000) and the length of these stretched fibers (54 nm), the distance between amino acid residues would be about 0.11 nm which is shorter than the distance found between the amino acid residues of any coiled-coil described so far [11].

REFERENCES

1. Crowter RA, Lenk EV, Kikuchi Y, King J: J Mol Biol 116:489–523, 1977.
2. Simon LD, Anderson TF: Virology 32:279–297, 1967.
3. Simon LD, Swan JG, Flatgaard JE: Virology 41:77–90, 1970.
4. Mason WS, Haselkorn R: J Mol Biol 66:445–469, 1972.
5. Zorzopulos J, Kozloff LM: J Biol Chem 253:5543–5547, 1978.
6. Kells SS, Haselkorn R: J Mol Biol 83:473–485, 1974.
7. Kells SS, Ohtsuki M, Haselkorn R: J Mol Biol 99:349–351, 1975.
8. Zorzopulos J, DeLong S, Chapman V, Kozloff LM: Proc 7th Biennial Bacteriophage Assembly Meeting, 1981, pp 341–351.
9. Adams MH: "Bacteriophages." New York: Interscience Publishers, Inc., 1959, pp 584–592.
10. Edgar RS, Wood WB: Proc Natl Acad Sci USA 55:498–505, 1966.
11. Fraser RDB, Mac Rae TP: "Conformation in Fibrous Proteins and Related Synthetic Polypeptides." New York: Academic Press, 1973.
12. Earnshaw WC, Goldberg EB, Crowther RA: J Mol Biol 132:101–131, 1979.
13. Small JV, Sobieszek A: J Cell Sci 23:243–268, 1977.
14. Edgar RS, Lielausis I: J Mol Biol 32:263–276, 1968.
15. King J, Mykolajewycz N: J Mol Biol 75:339–358, 1973.
16. Yamamoto M, Uchida H: Virology 52:234–245, 1973.
17. Kozloff LM: Proc 7th Biennial Bacteriophage Assembly Meeting, 1981, pp 327–342.
18. Beck BD, Arscott PG, Jacobson A: Proc Natl Acad Sci USA 75:1250–1254, 1978.
19. Neimark HC: Proc Natl Acad Sci USA 74:4041–4045, 1977.
20. Allen ED, Sussman AS: J Bacteriol 135:713–716, 1978.
21. Townsend R, Archer DB, Plaskitt KA: J Bacteriol 142:694–700, 1980.
22. Minkoff L, Damadian R: J Bacteriol 125:353–365, 1976.
23. Wang E, Wolf BA, Lamb RA, Chopin PW, Goldberg AR: In Goldman R, Pollard T, Rosenbaum J (eds): "Cell Motility." Cold Spring Harbor, NY: Cold Spring Harbor Press, 1976, pp 589–600.
24. Moore PB, Huxley HE, De Rosier DJ: J Mol Biol 50:279–295, 1970.
25. Johnson P, Peny SV: J Biochem 110:207–216, 1968.
26. McKee PA, Rogers LA, Mosler E, Hill RL: Arch Biochem Biophys 116:271–279, 1966.